

53  
4-19-93 JS②

CONF 920913--29

PREPARED FOR THE U.S. DEPARTMENT OF ENERGY,  
UNDER CONTRACT DE-AC02-76-CHO-3073

PPPL-2891  
UC-420,426

PPPL-2891

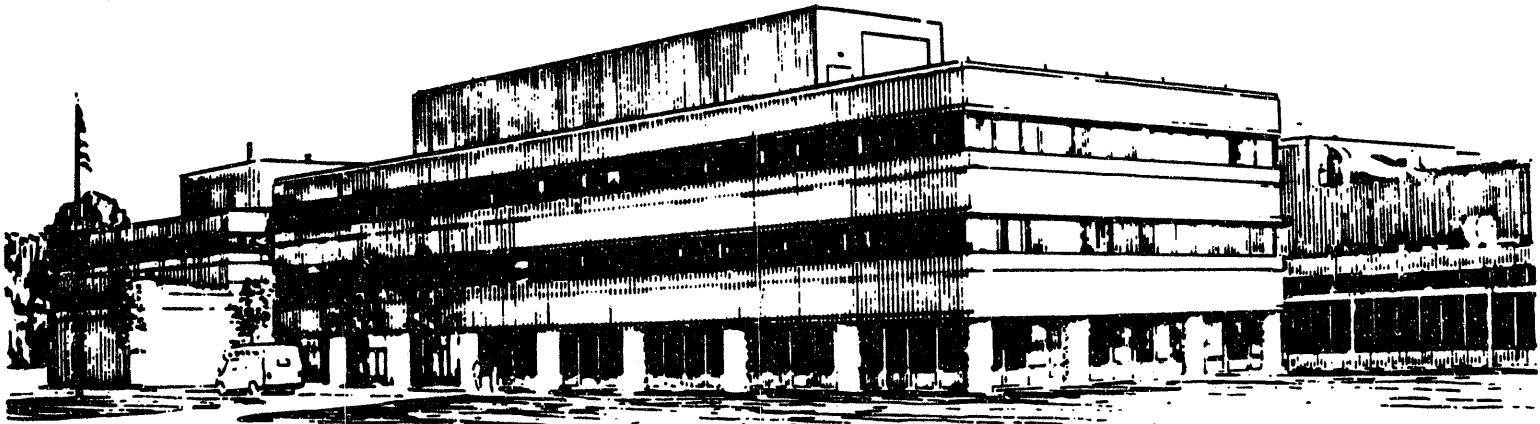
CHARGED FUSION PRODUCT AND FAST ION LOSS IN TFTR

BY

S.J. ZWEBEN, R. BOIVIN, D.S. DARROW, ET AL.

MARCH, 1993

PRINCETON  
PLASMA PHYSICS  
LABORATORY



PRINCETON UNIVERSITY PRINCETON NEW JERSEY

## **NOTICE**

This report was prepared as an account of work sponsored by an agency of the United States Government. Neither the United States Government nor any agency thereof, nor any of their employees, makes any warranty, express or implied, or assumes any legal liability or responsibility for the accuracy, completeness, or usefulness of any information, apparatus, product, or process disclosed, or represents that its use would not infringe privately owned rights. Reference herein to any specific commercial produce, process, or service by trade name, trademark, manufacturer, or otherwise, does not necessarily constitute or imply its endorsement, recommendation, or favoring by the United States Government or any agency thereof. The views and opinions of authors expressed herein do not necessarily state or reflect those of the United States Government or any agency thereof.

## **NOTICE**

This report has been reproduced from the best available copy.  
Available in paper copy and microfiche.

Number of pages in this report: 21

DOE and DOE contractors can obtain copies of this report from:

Office of Scientific and Technical Information  
P.O. Box 62  
Oak Ridge, TN 37831;  
(615) 576-8401.

This report is publicly available from the:

National Technical Information Service  
Department of Commerce  
5285 Port Royal Road  
Springfield, Virginia 22161  
(703) 487-4650

This is a preprint of a paper presented at the  
Fourteenth International Conference on Plasma  
Physics and Controlled Nuclear Fusion Research,  
September 30 through October 7, 1992 in  
Wurzburg, Germany.

MASTER

EP



INTERNATIONAL ATOMIC ENERGY AGENCY

FOURTEENTH INTERNATIONAL CONFERENCE ON PLASMA  
PHYSICS AND CONTROLLED NUCLEAR FUSION RESEARCH

Würzburg, Germany, 30 September – 7 October 1992

IAEA-CN-56/A-6-3

**CHARGED FUSION PRODUCT AND FAST ION LOSS  
IN TFTR**

S.J. ZWEBEN, R. BOIVIN<sup>1</sup>, D.S. DARROW, E.D. FREDRICKSON, H.E.  
MYNICK, R.B. WHITE, H. BIGLARI, N. BRETZ, R. BUDNY, C.E.  
BUSH, C.S. CHANG, L. CHEN, C.Z. CHENG, R. FISHER<sup>2</sup>, R.  
FONCK<sup>3</sup>, G.-Y. FU, G.W. HAMMETT, R.J. HAWRYLUK, J. HOSEA, L.  
JOHNSON, J. S. MACHUZAK<sup>1</sup>, J. Mc CHESNEY<sup>2</sup>, D. MANSFIELD, K.  
McGUIRE, G. McKEE<sup>3</sup>, S.S. MEDLEY, R. NAZIKIAN, D.K. OWENS, H.  
PARK, J. PARK, C.-K. PHILLIPS, J. SCHIVELL, B.C. STRATTON, M.  
TUSZEWSKI<sup>4</sup>, M. ULRICKSON, R. WILSON, P. WOSKOV<sup>1</sup>, K.M.  
YOUNG

Plasma Physics Laboratory,  
Princeton University,  
Princeton, N.J.,  
United States of America

**Abstract**

**CHARGED FUSION PRODUCT AND FAST ION LOSS IN TFTR**

Several different fusion product and fast ion loss processes have been observed in TFTR using an array of pitch angle, energy and time resolved scintillator detectors located near the vessel wall. For D-D fusion products (3 MeV protons and 1 MeV tritons) the observed loss is generally consistent with expected first-orbit loss for  $I_p < 1.4$  MA, except near the outer midplane where stochastic TF ripple loss dominates when  $I_p > 1$  MA. However, at higher currents,  $I_p = 1.4$ -2.5 MA, an MHD induced D-D fusion product loss can be up to 3-4 times larger than the first-orbit loss, particularly at high beam powers,  $P \geq 25$  MW. The MHD induced loss of 100 KeV neutral beam ions and  $\approx 0.5$  MeV ICRF minority tail ions has also been measured  $\leq 45^\circ$  below the outer midplane. The potential implications of these results for D-T alpha particle experiments in TFTR and ITER are described.

<sup>1</sup> Massachusetts Institute of Technology, Cambridge, Mass. USA

<sup>2</sup> General Atomics, San Diego, California, USA

<sup>3</sup> University of Wisconsin, Madison, Wisconsin, USA

<sup>4</sup> Los Alamos National Laboratory, Los Alamos, New Mexico, USA

## 1. Introduction:

Good confinement of the fusion product alpha particles born at 3.5 MeV in D-T is essential for efficient and predictable alpha heating of future tokamak reactors. In addition, the unanticipated loss of only a few percent of the fast alpha population could potentially damage the first wall or divertor structure, since these fast alphas will contain  $\approx 10\text{-}30\%$  of the total stored plasma energy, and this energy loss might be highly localized, or might occur on a faster timescale than the thermal plasma loss.

This paper describes measurements of the loss of D-D fusion products and other fast ions in TFTR, and discusses the implications of these results for the TFTR D-T experiment and for an ITER-sized D-T tokamak. Since the D-D fusion product population is very small ( $<10^{-4}$  of the total ion density), the present measurements mainly concern "single-particle" loss mechanisms, which will most likely persist in future tokamaks, even without collective fast particle instabilities[1]. Previous studies in TFTR have shown that classical first-orbit loss is the dominant D-D fusion product loss mechanism in MHD-quiet plasmas at  $R \approx 2.6$  m, and that diffusion of D-D fusion products across the passing/trapped boundary is small[2]. Here we concentrate on other loss mechanisms which may be more relevant for high current plasmas like ITER, such as those caused by toroidal field ripple, MHD activity, and ICRF heating.

Most of the experimental results are obtained from the "lost alpha" diagnostic, which measures escaping fast ions with gyroradii in the range  $11 \text{ cm} \geq \rho \geq 2 \text{ cm}$ , e.g. D-D fusion product protons and tritons with  $\rho \approx 5 \text{ cm}$  at 5 T. Three detectors are fixed at poloidal angles of  $45^\circ$ ,  $60^\circ$  and  $90^\circ$  below the outer midplane of the vacuum vessel a few centimeters outside the geometrical shadow of toroidally displaced "RF limiters" (the plasmas may be displaced in major radius with respect to the vessel center). A fourth detector is mounted on a movable probe  $20^\circ$  below the outer midplane. Experimental details and calibrations are described elsewhere[2-4].

## 2. Stochastic TF Ripple Loss of D-D Fusion Products:

The radially movable detector located  $20^\circ$  below the outer midplane was designed to measure stochastic toroidal field (TF) ripple induced loss of D-D fusion products[5,6]. In theory, this mechanism causes the banana tips of fast trapped ions to diffuse vertically, such that they should be lost to the wall just below the outer midplane[7]. In TFTR, the stochastic threshold for D-D fusion products occurs outside a poloidal circle of radius  $r \approx 0.5$  m centered at  $R = 2.2$  m, where the ripple strength is  $\delta > 0.02\%$ [3]. Note that this mechanism does not involve trapping inside the local TF ripple wells, but rather the diffusion of normal banana trapped ions.

The first experimental indication of stochastic TF ripple diffusion came from the pitch angle distribution measured when the probe aperture was  $\approx 4.5$  cm behind the geometrical shadow of the RF limiter radii ( $120^\circ$  and  $170^\circ$  counter toroidally). Two well-resolved peaks were observed for an  $R = 2.6$  m plasma at  $I_p = 1.4$  MA, as shown in Fig. 1(a). The location of the lower peak at a pitch angle of  $\chi \approx 55^\circ$  (with respect to the co-toroidal direction) matches the expected first-orbit loss, while the location of the larger peak at

$\chi \approx 62^\circ$  cannot be explained by first-orbit loss, but agrees fairly well with the expected location of stochastic TF ripple loss having banana tips below the plasma center, as calculated by hybrid mapping/guiding center Monte Carlo code MAPLOS[3].

The ratio between the observed peak heights does not quite agree with the model, and a better fit to the data can be obtained with an *ad hoc* coefficient of  $\approx 2$  multiplying the original stochastic threshold[3]. However, there are also uncertainties of this order due to the modeling of the limiter geometry and the  $q(r)$  profile, which are not yet fully taken into account. At higher currents the high-pitch angle peak increases with respect to the first-orbit loss peak, as expected from the ripple loss model, since first-orbit loss decreases more rapidly with current. At lower currents ( $\leq 1$  MA) the high-pitch angle peak is smaller than the first-orbit loss peak as expected, since most D-D fusion products are then lost on their first orbit.

In a second experiment the detector was scanned radially in an  $I_p = 1.6$  MA plasma with  $R = 2.45$  m to measure the "scrape-off" width of D-D fusion products in the shadow of the RF limiter, with the result shown in Fig. 1(b). A simple random walk model was used to interpret this data in terms of the radial step size per bounce,  $\Delta r$ , for these confined trapped ions measured in the shadow of the RF limiters, resulting in the model curves shown in Fig. 1(b). The best fit to the data is for  $\Delta r = 0.65$  cm, which is in good agreement with the expected TF stochastic ripple step size of  $\Delta r = 0.75 \pm 0.2$  cm for D-D fusion product ions in the region of these banana tips. Separate measurements of radial diffusion in the shadow of a second movable probe also imply a vertical step size  $\Delta r \approx 0.5$  cm/bounce, roughly consistent with the Goldston-White-Boozer model[3,5].

The escaping ion energy determined from the measured gyroradius distributions for these cases was very near to the birth energy of these D-D fusion products. This is also consistent with the MAPLOS calculation for TF stochastic ripple loss, which show a mean loss time of only  $\approx 3$  msec, which is small compared to the thermalization time of  $\approx 0.2$  sec. Note that the results of Fig. 1 were taken at relatively low beam power (11 MW and 19 MW, respectively) in discharges without strong coherent MHD activity (see Sec. 3).

### 3. Anomalous Loss Processes:

One measure of the MHD induced D-D fusion product loss can be determined by comparing the total loss to the  $90^\circ$  detector (integrated over pitch angle and gyroradius and normalized to the neutron rate) with the expected first-orbit loss, as done in Fig. 2(a) for a set of about 200 TFTR discharges. These plasmas had a major radius of  $R = 2.45$  m, a minor radius of  $a = 0.8$  m, a toroidal field of  $B = 5.0 \pm 0.2$  T, and a neutral beam injection (NBI) power of  $P = 5-32$  MW. There are evidently many cases in which the total loss at  $90^\circ$  is significantly larger than that expected from the first-orbit loss model (TF ripple loss is not expected at  $90^\circ$ ). The first-orbit loss curve is normalized to the data at  $I_p = 0.7$  MA where the first-orbit loss is expected to be dominant, since the banana widths are larger than the plasma radius[2].

Figure 2(b) shows this same fusion product loss rate plotted vs. NBI

power for the  $I_p = 1.80-1.85$  MA cases of Fig. 2(a). There are apparently two types of anomalies: one in which the loss gradually increases by a factor of  $\approx 2$  between 20-32 MW (corresponding to  $0.5-3.3 \times 10^{16}$  neutrons/sec), and the other in which it can increase to up to a factor of 3-5 above the first-orbit loss, even at relatively low beam power. For the latter cases the increased loss is clearly modulated by strong coherent MHD activity (Sec. 3.1), while it is not for the cases which show a gradual increase in loss with NBI power (Sec. 3.3).

The global loss corresponding to these anomalies can not be easily determined, since these detectors measure only four points on a large and complex limiter/wall surface, and since their absolute calibration is uncertain to within a factor of 2-3. However, rough estimates can be made based on the observed increase above the first-orbit level at  $90^\circ$ , assuming that the spatial distribution of the anomalous loss is similar to that of the first-orbit loss. Since the total loss to the bottom detector during strong MHD activity at 1.8 MA can rise up to the first-orbit loss level at  $\approx 0.8$  MA, which is  $\approx 20\%$  globally[3], then the maximum MHD-induced loss can be estimated to be  $\approx 10-30\%$  globally. For the other type of anomaly the total loss at the bottom is about twice the first-orbit loss level at 1.8 MA, which is in the range of a few percent; therefore this loss can be estimated to be  $\approx 1-10\%$  globally.

### 3.1 Coherent MHD-Induced Loss

A typical case of coherent MHD induced D-D fusion product loss is illustrated in Fig. 3(a), which shows the loss vs. time at the  $90^\circ$  detector for an  $I_p = 1.4$  MA discharge with  $P = 24$  MW, as monitored by a photomultiplier (PM) tube with a frequency response of up to  $\approx 20$  kHz. Here the D-D fusion product signal is normalized to the neutron rate vs. time for another discharge in the same sequence without MHD activity (at  $P = 20$  MW). Thus the MHD activity after 3.5 sec increases the fusion product loss by about a factor of 2 above the MHD-quiescent case. Qualitatively similar MHD induced loss is observed over the range  $I_p = 1.0-2.5$  MA in TFTR.

This increased fusion product loss is modulated at the frequency of the  $\approx 0.5$  kHz MHD activity, as shown in Fig. 3(b). In this discharge there was strong  $m = 2, n = 1$  and  $m = 1, n = 1$  MHD activity starting at  $\approx 3.5$  sec, with a typical (2,1) level estimated from the Mirnov signals to be  $\bar{B}_r/B_T \approx 3 \times 10^{-4}$  near the  $q \approx 2$  surface at 3.6 sec. This type of MHD induced fusion product loss has previously been observed for other types of coherent modes over a wide frequency range ( $\approx 1$  Hz-10 kHz)[8], e.g. during fishbone-like  $m=1, n=1$  MHD activity, in which the loss increases along with bursts of MHD activity, and during H-modes[9], when the loss often shows rapid spikes correlated with ELMS. Similar MHD induced loss is seen in the the other escaping fusion product detectors.

### 3.2 Other MHD and ICRF Induced Loss

Sawtooth crashes are often accompanied by sudden bursts of D-D fusion product loss lasting  $\approx 0.1-1$  msec which are briefly up to 2-4 times higher than the first-orbit loss level, such as shown for the  $90^\circ$  detector in Fig. 4(a). These bursts are localized near the pitch angle of the passing/trapped boundary (as if passing ions near  $q = 1$  were being radially transported at the crash), and can be seen on all detectors. Fusion product loss can also increase

dramatically prior to a major disruption, as shown in Fig. 4(b), where the instantaneous loss rate increases by over a factor of 50 during the pre-disruptive period (2.80-2.84 sec). This is most likely due to the large pre-disruptive MHD activity, which in this case involves an  $m = 2$ ,  $n = 1$  locked mode[10].

The global loss fraction for confined fusion products during these two types of events can be estimated from the instantaneous loss rate (normalized by the expected first-orbit loss rate of  $\approx 5\%$ ) times the ratio of the duration of the increased loss divided by the fusion product slowing-down time ( $\approx 0.2$  sec). Thus at each sawtooth crash, during which the loss rate increases by a factor of 2 over  $\approx 100$   $\mu$ sec, the loss fraction is only  $\approx (2 \times 5\%) \times (0.1 \text{ msec} / 200 \text{ msec}) \approx 10^{-4}$ ; however, for the pre-disruptive loss the corresponding loss fraction is  $\approx 1-10\%$ . Note that these estimates make the oversimplified assumption that the poloidal loss distribution during these events is the same as it is for the first-orbit loss, which is not necessarily the case.

MHD induced loss of neutral beam and ICRH minority tail has also been observed using the same detectors. In these cases the MHD activity might be driven by the fast ions themselves, since their population is  $>100$  times larger than the D-D fusion product populations described above. For example, bursts of 100 keV beam ion loss have been observed in the outer midplane detector during high frequency magnetic fluctuations identified with TAE modes, as described elsewhere[11]. Also, during the Axisymmetric Beam-Driven Mode (ABM)[12], which is thought to be another beam-driven MHD mode, a loss of 100 keV beam ions has been observed at similar fields ( $B=1.5$  T,  $I_p = 0.5$  MA), but at even lower NBI power ( $P \approx 2$  MW), as shown in Fig. 4(c). This type of beam ion loss coincides with magnetic fluctuations at 30 and 50 kHz, i.e. much lower than the expected TAE frequency. The detected beam ions have a pitch angle of  $\chi \approx 50^\circ$ , corresponding to loss of trapped ions near the passing/trapped boundary. Since most of the beam ions are injected on passing orbits, the implication is that the MHD activity transports some of these ions until they are trapped and lost.

Various types of ICRF induced MeV ion loss have been observed on TFTR. During H minority heating above  $\approx 2-3$  MW (without NBI) a clear H tail loss is observed, mainly in the detectors at  $45^\circ$  and  $20^\circ$  below the outer midplane at an energy of  $E \approx 0.5 \pm 0.2$  MeV and a pitch angle corresponding to trapped ion orbits with banana tips  $\approx 0.8$  m below the plasma center. The estimated tail ion power loss is  $\approx 0.1$  MW at an ICRF power of 4 MW, i.e.  $\approx 1-10\%$  of the ICRH power (assuming that loss is uniform  $\leq 45^\circ$  below the outer midplane). This anomalous loss can be strongly modulated by MHD activity; for example, it often has a large decrease in phase with the central soft x-ray signal, and can be modulated by  $m=2$  modes and sawtooth crashes (which can produce a spike similar to that for D-D fusion products). This may also be related to high frequency instabilities observed recently in similar ICRH-only discharges[13].

During  $^3\text{He}$  minority heating an anomalously large loss is also observed in the  $45^\circ$  detector, along with the first-orbit loss of D- $^3\text{He}$  alphas in all detectors[14]. However, this anomalous signal is at a gyroradius just below that of the D-D or D- $^3\text{He}$  fusion products, leading to the suspicion that it is not due to tail ion loss, but rather to ICRF induced deconfinement of fusion products. Additional evidence for the latter process is shown in Fig. 4(d),

which shows the 90° detector signal for an ICRF electron heating experiment with NBI but without any minority tail species. This increased loss observed with ICRF can (so far) only be understood as ICRF induced deconfinement of one of the D-D fusion products, possibly the 1 MeV triton (due to its second harmonic resonance). Note that in this case the other PM detectors did not show increased loss, thus eliminating the possibility of RF pickup.

The present uncertainty concerning the mechanisms of these ICRF induced ion losses leaves open the possibility that D-T alphas could be deconfined by ICRH in TFTR or ITER. However, these processes might eventually be useful as a means for alpha particle burn control or ash removal.

### 3.3 New Anomalous Delayed Loss of Trapped Fusion Products

A new feature of D-D fusion product loss has been observed at plasma currents  $I_p = 1.4 - 2.5$  MA and NBI powers of  $P = 7-32$  MW in discharges with relatively small plasma major radii of  $R \approx 2.40-2.50$  m[15]. The scintillator patterns in this range shows a persistent high- $\chi$  loss feature, as illustrated in Fig. 5(b), which increasingly dominates the 90° detector signal as the plasma current and beam power are increased. This feature appears to be superimposed on the usual first-orbit loss, which dominates the signal at low currents, as shown in Fig. 5(a). The anomalous loss feature remains near  $\chi \approx 70^\circ$  in this current range, whereas the first-orbit feature shifts to lower  $\chi$  with increased current, as expected and also observed for  $I_p < 1.4$  MA and for  $R = 2.6$  m plasmas[2,8].

This new feature caused the gradual increase in the total loss with increasing NBI power shown in Fig. 2(b), and was largely responsible for the somewhat higher than expected normalized fusion product loss in the range  $I_p = 1.6-2.5$  MA (in the absence of strong MHD activity) shown in Fig. 2(a). This type of anomalous loss increased relative to the first-orbit loss with increasing plasma current, and was about equal to the first orbit loss at  $I_p = 2$  MA. Note that this feature was not accompanied by observable MHD induced modulation of the D-D fusion product loss signal.

At  $I_p = 2$  MA the gyroradius distribution of the total loss to the bottom detector corresponded to an average ion energy of  $E/E_0 \approx 55\% \pm 15\%$  compared to the birth energy  $E_0$  expected for D-D fusion products, as shown in Fig. 5(c). This surprisingly low energy was correlated with the observed time dependence of the anomalous feature at high pitch angle, which was delayed by  $\approx 0.1-0.2$  sec with respect to the prompt first-orbit loss at the beginning of NBI, and which persisted  $\approx 0.1-0.2$  sec after the first-orbit loss feature disappeared at the end of NBI. This corresponds to the time needed for D-D fusion products to collisionally thermalize to about half of their birth energy.

This combination of anomalously high  $\chi$  and low  $E/E_0$  for D-D fusion products (lost at 90°) implies that the last confined orbit was deeply trapped, with its banana tip  $\approx 0.8$  m below the plasma center (i.e. not near the passing/trapped boundary). In order for such an orbit to have missed the outer limiter, its banana tip must have had a vertical displacement of  $> 10$  cm over its last bounce, which is larger than the  $\approx 3$  cm vertical step expected from stochastic TF ripple diffusion for a banana tip located at the plasma edge (see

Sec. 2). The mechanism for this large last step size is not known.

This new anomalous delayed loss feature could also be modulated during strong MHD activity, sometimes increasing, as in Fig. 3(a), but also sometimes disappearing during the same discharge, leaving only the first-orbit loss feature. This suggests that this new feature might be due to some magnetic perturbation which is outside the frequency range of detection for escaping fusion products (which is  $\approx 1$  Hz-20 kHz), but which is very reproducible shot-to-shot (in contrast with the normal low- $m$  MHD activity). Another possibility is that this delayed loss might be due (in part) to TF ripple, perhaps enhanced by slightly misaligned TF coils; however, the disappearance of delayed loss at  $90^\circ$  detector for large-ripple plasmas with  $R = 2.6$  m is difficult to understand.

### 3.4 Modeling of MHD-Induced Fusion Product Loss

The MHD-induced fusion product losses described in Secs. 3.1-3.2 are presumably caused by internal plasma-driven magnetic perturbations, which can be considered static with respect to the fusion product transit frequency of  $\approx 1$  MHz. This mechanism has been modeled using a fast and accurate guiding-center Monte-Carlo orbit code[16] which includes the effects of stationary low- $n$  helical magnetic islands. It has recently been shown analytically that a stochastic threshold for both trapped and passing ions exists when the shift of the high energy orbits from the magnetic flux surfaces is comparable to the perpendicular wavelength of the mode[17].

A test case for TFTR was chosen with  $I_p = 2$  MA and  $B = 5$  T in a plasma with  $R = 2.45$  m,  $a = 0.8$  m and a limiter centered at  $R = 2.61$  m and  $a = 0.99$  m, i.e. similar to the 1.8 MA discharges of Fig. 2. For each run of the code 300 alpha particles (with orbits very similar to D-D fusion products) were started at random positions and magnetic moments with a radial source profile  $\propto (1 - [(r/a)^2]^\beta)$ , and were followed for 3000 poloidal transits at a fixed energy and magnetic moment, corresponding to a real time of  $\approx 10$  msec for 3.5 MeV alphas. A zero-beta equilibrium with a parabolic  $q(r)$  profile was used with  $q(0)=1$  [except for the (1,1) case when  $q(0) = 0.8$ ], assuming a parabolic  $q(r)$  profile (probably somewhat broader than that in TFTR). No toroidal field ripple was present, and the alphas were assumed to be collisionless.

The total loss fraction for alphas at  $E_0 = 3.5$  MeV for various assumed perturbations are shown in Fig. 6(a), where the perturbation is specified by the maximum  $\bar{\delta}_r/B_T$  near the mode rational surface. For single-helicity modes with  $(m,n)=(1,1)$ , (2,1), and (3,2) the MHD-induced loss becomes comparable to the first-orbit loss level ( $\approx 5\%$  at  $\bar{\delta}_r/B_T=0$ ) at a perturbed field strength of  $\bar{\delta}_r/B_T \approx 3 \times 10^{-3}$ , and the loss fraction rises approximately linearly with  $\bar{\delta}_r/B_T$  above this threshold. This level of perturbation corresponds to a rather large (2,1) island half-width of  $\delta r/a \approx 0.15$ , which scales as  $\delta r/a \propto (\bar{\delta}_r/B_T)^{1/2}$ . Note that for the (2,1)+(3,2) case the horizontal axis refers only to the (2,1) mode strength, to which was added a (3,2) mode with a maximum amplitude  $\approx 1.6$  times that of the (2,1). These results are at least qualitatively similar to previous Monte Carlo calculations for TAE modes in CIT[18] and single  $(m,n)$  modes in NET[19].

Examination of the orbit trajectories for these runs shows that there are three basic MHD-induced loss processes[20]: (a) trapped particle diffusion with loss just below the outer midplane, (b) co-going passing ion diffusion with loss just below the outer midplane, and (c) counter-going passing ion diffusion with loss either near the inner midplane, or across the passing-trapped boundary to the bottom of the vessel. For runs with a moderate level of total loss (<30%), almost all of the calculated loss occurs within  $\approx 30^\circ$  of the outer midplane, with <10% of the total loss occurring near the vessel bottom at  $90^\circ$ .

The effect of varying the assumed alpha energy for this  $I_p = 2$  MA case is shown in Fig. 6(b). The calculated MHD-induced loss fraction decreased with decreasing ion energy for all cases examined. For example, the (2,1) case

which had  $\approx 16\%$  loss for  $E_0 = 3.5$  MeV alphas had only  $\approx 1\%$  loss for  $E = 0.6$  MeV alphas. Note that for  $E/E_0 < 0.5$  there is very little first-orbit loss (<1%), and so most of the loss at the lower energies is due to the MHD effect.

The connection between these calculations and the observed MHD-induced losses is not yet clear. The observed MHD induced loss at  $90^\circ$  is comparable to the local first-orbit loss at an estimated  $\bar{B}_r/B_T$  about 5-10 times lower than expected from this global loss modeling (assuming a single mode), and the calculated loss is mainly near the outer midplane, not at  $90^\circ$ [20]. Also, the calculations do not show any increased loss near  $E/E_0 \approx 0.5$ , which might have explained the delayed loss feature of Sec. 3.3. However, it is possible that a combination of various (m,n) modes can reduce the peak  $\bar{B}_r/B_T$  needed for a given amount of loss, as suggested recently[21], and as seen for the (2,1)+(3,2) case in Fig. 6(b). Note that the present model does not yet include the  $\nabla \bar{B}$  terms in the alpha drifts, but only the  $v_{||} \bar{B}_r/B_T$  terms. These two effects can be comparable for MeV ions near the magnetic islands; therefore including the new terms could significantly increase the local diffusion rate, and may improve the comparison with experiment.

#### 4. Implications for D-T Alpha Particle Experiments:

These D-D fusion product and fast ion loss measurements form a baseline data set which can be used to evaluate the alpha particle loss observed during the TFTR D-T experiment. The D-T fuel will increase the fusion product populations by a factor of  $\approx 100$ [22], thereby allowing several new possibilities which should contribute to an assessment of alpha physics in ITER, such as direct measurements of the confined alpha populations and a search for collective alpha instabilities.

##### 4.1 Confined Alpha Measurements

The expected D-T alpha particle distributions inside the plasma have been calculated using a new alpha simulation code MIDD[23], which includes the radial birth profile and creation rate vs. time, the classical thermalization process, and a variable *ad hoc* radial diffusion coefficient  $D$  (assumed to be independent of alpha energy). Typical results for a standard supershot case [as in Ref. 22] show that: (a) the central density of partially thermalized alphas

(100-400 keV) reaches a maximum only at the end of the 1 sec NBI pulse, due to the  $\approx 0.5$  sec time-to-peak of the D-T reaction rate and the  $\approx 0.5$  sec thermalization time for alphas (assuming  $D=0$ ), (b) a relatively small  $D=0.1$   $\text{m}^2/\text{sec}$  causes the central density of 100-400 KeV alphas to decrease by a factor of  $\approx 3$  after 1 sec (compared to  $D = 0$ ), and (c) a  $D = 0.5$   $\text{m}^2/\text{sec}$  is sufficient to cause inversion of the on-axis alpha energy distribution below  $\approx 2.5$  MeV.

Simulations such as these will be used to interpret the results from the confined alpha particle diagnostics which are being planned for the TFTR D-T run. These measurements should include: (a) the alpha source profile, as determined by a 10-channel vertical neutron profile monitor[24], (b) the partially thermalized alpha energy spectrum up to  $\approx 1$  MeV, as determined by a 5-channel alpha CHERS system[25], (c) the alpha energy spectrum up to  $\approx 3.5$  MeV, as determined by charge exchange neutral measurements made in a Li pellet ablation cloud[26], and (d) the alpha spectrum up to over 3.5 MeV vs. radius using a 60 GHz gyrotron scattering technique[27]. These confined alpha diagnostics will be supplemented by the escaping alpha diagnostic (essentially as described above), and extensive fluctuation diagnostics for alpha instability studies.

#### 4.2 Search for Collective Alpha Instabilities

A major goal of the TFTR D-T run is to identify potential collective alpha instabilities such as the toroidal Alfvén eigenmode (TAE), the kinetic ballooning mode (KBM), alpha fishbones, and/or alpha driven sawteeth or sawtooth stabilization. These D-T experiments should ideally be performed during periods with high alpha populations but without large plasma-driven MHD activity, since such MHD activity can also cause alpha loss and/or change the confined alpha distribution (Sec. 3). The alpha transport effects of any collective modes can then be evaluated from the measurements of the alpha source profile and the confined and lost alpha populations.

The most recent calculations of TAE stability in TFTR D-T discharges show that the expected alpha populations in high power supershots are about a factor of 2-5 below the estimated  $\beta_\alpha$  threshold for  $n = 1$  TAE instability[22,28,29]. Ion Landau damping is the dominant stabilizing effect in these cases, which suggests that TAE modes may be more unstable shortly after NBI begins and ends (due to the lower plasma ion beta), or during the steady state of lower power supershot discharges[28]. The most recent calculations of KBM stability for TFTR D-T discharges show that the  $\beta_\alpha$  in high power supershots is about a factor of 5 below the expected threshold for  $n = 3-5$  KBM excitation, even though these discharges are near the first stability boundary[30].

It should be noted that the presence of ICRH minority tail ions will probably affect the collective alpha stability, since these ions have a similar energy spectrum and an even higher fast particle beta than the D-T alphas. In fact, there is recent evidence of a ICRH tail ion-driven collective instability in D-D discharges[13].

### 4.3 Possible Implications for ITER:

Rough estimates of alpha loss in ITER can be made from these TFTR results after correcting for the expected changes in the dimensionless alpha parameters such as  $\beta_\alpha$  and  $\rho_\alpha/a$  (alpha gyroradius/minor radius). Note that the allowable alpha energy loss fraction in ITER may be as low as  $\approx 1\%$ , due to the possibility of localized alpha heat loads on first wall components[31].

The measurements of midplane D-D fusion product loss (Sec. 2) are so far consistent with the stochastic TF ripple diffusion theory [5,6], at least to within a factor of two in the threshold ripple strength[3]. Thus the ITER alpha loss rate of  $\leq 1\%$  calculated using this theory should be correct[31]. However, the vertical elongation in ITER causes the escaping alphas to be trapped in the local ripple wells[31], a process which has not been evaluated in TFTR.

The MHD-induced losses described in Sec. 3.1 should be equivalent in devices which have the same  $\rho_\alpha/a$ , which determines the alpha particle orbit structure for a fixed  $\delta r/a$  (island width),  $q(r)$  and  $R/a$ [17]. Thus the loss of  $E_0 = 3.5$  MeV alphas for a 5 T (circular) machine with  $a=2$  m should be equivalent to that for alphas in TFTR at  $E \approx (0.8/2.0)^2 E_0 \approx 0.6$  MeV. Since the MHD-induced loss fraction of near-birth energy D-D fusion product ions in TFTR can be up to  $\approx 10-30\%$  (i.e. four times the expected first-orbit loss of  $\approx 5-10\%$  at 1.8 MA), and the calculated alpha loss at  $\approx 0.6$  MeV is  $\approx 5-10\%$  that of 3.5 MeV alphas [Fig. 6(b)], then the inferred loss for 3.5 MeV alphas in ITER is only  $\approx 1-3\%$  for a similar MHD mode. Obviously this is only a very crude estimate, particularly since this model has not yet explained the observed loss. However, alpha loss in ITER might be larger for MHD modes with a wide spectrum of (m,n) values, or modes which resonate with the alphas[18,28].

The pre-disruptive and delayed D-D fusion product losses measured at  $90^\circ$ , as shown in Figs. 4 and 5, suggest that added protection for the wall and/or divertor plates may be needed in ITER in the ion  $\nabla B$  drift direction. Note that the total loss at  $90^\circ$  for MHD-quietest  $R = 2.45$  m plasmas does not significantly decrease between  $I_p = 1.4$  MA and 2.5 MA (Fig. 2), mainly due to the delayed loss component at the higher currents. If this trend persists to even higher currents there may be up to a few-% delayed alpha loss in ITER. However, if this process could be understood and controlled, it might eventually prove useful for epithermal ash removal.

### 5. Summary and Conclusion:

Several D-D fusion product loss mechanisms have been examined in TFTR using an array of escaping fast ion detectors. Near the outer midplane a loss of trapped fusion product ions has been observed which is consistent with the theoretically-predicted stochastic TF ripple loss. At the vessel bottom the loss can increase to up to a factor of  $\approx 3-5$  above the expected first-orbit loss level during large coherent plasma-driven MHD activity. Other non-classical loss processes which have been observed include a new delayed loss of trapped D-D fusion products at about half their birth energy, and an ICRF induced loss of minority tail ions and possibly fusion products.

Table 1 gives a list of these "single-particle" loss mechanisms along with rough estimates for the global alpha loss expected for them during the TFTR D-T experiment and for ITER, based on these experimental results supplemented by the modeling and theory described above. Although presently only order-of-magnitude estimates, these results do suggest that global alpha heating in a high-current tokamak like ITER will probably not be seriously degraded by single particle loss processes. This is consistent with the generally good heating efficiency observed with high energy ions, and with previous fast ion confinement measurements in TFTR[32] and JET[33,34].

However, several of these mechanisms could result in  $\approx 1\%$  alpha energy loss, which is potentially enough to cause localized damage to the first wall or divertor plate of ITER (i.e.  $>2$  MW). Therefore, more work needs to be done to evaluate the physical mechanisms and spatial distribution of these losses (poloidally, toroidally and radially). If this can be accomplished, along with the avoidance of collective alpha instabilities in D-T, then efficient and predictable alpha heating is likely to be obtained in ITER.

**Acknowledgments:** We thank H.P. Furth, D.M. Meade, D.J. Sigmar, and particularly J.D. Strachan for their consistent support for these measurements on TFTR. This work was performed under DoE contract No. DE-AC02-CHO-3073.

### **References:**

- [1] FURTH, H.P., et al, Nucl. Fus. **30**, 1799 (1990)
- [2] ZWEBEN, S.J., BOIVIN, R.L., CHANG, C.-S., et al, Nucl. Fus. **31**, 2219 (1991).
- [3] BOIVIN, R.L. et al, Rev. Sci. Inst. **63**, 4418 (1992); Princeton Plasma Physics Laboratory Report PPPL-2797 (1991)
- [4] TUSZEWSKI, M., et al, Rev. Sci. Inst. **63**, 4542 (1992)
- [5] GOLDSTON, R.J., WHITE, R.B., and BOOZER, A.H., Phys. Rev. Lett. **47**, 647 (1981)
- [6] WHITE, R.B., MYNICK, H.E., Phys. Fluids **B1**, 980 (1989)
- [7] GOLOBOROD'KO, V. Y. and YAVORSKIJ, V.A., Nucl. Fus. **29**, 1025 (1989)
- [8] ZWEBEN, S.J., Boivin, R.L., DIESSO, M., et al, Nucl. Fus. **30**, 1551 (1990)
- [9] BUSH, C.E., et al, Princeton Plasma Physics Laboratory Report PPPL-2863 (1992)
- [10] JANOS, A., et al, this conference
- [11] DARROW, D.S. et al, Proc. 19th European Physical Society Conference on Plasma Physics, Innsbruck, page I-431, 1992
- [12] FREDRICKSON, E.D., et al, in Proc. 16th European Conference on Plasma Physics, Venice, 1989, Part 2, p. 481.
- [13] WILSON, J. R. , et al, this conference
- [14] ZWEBEN, S.J., HAMMETT, G.W., BOIVIN, R.L., et al, Nucl. Fusion **32**, 1823 (1992)
- [15] ZWEBEN, S.J., et al, Princeton Plasma Physics Laboratory Report PPPL-2864 (1993)
- [16] WHITE, R.B. and CHANCE, M.S., Phys. Fluids **27**, 2455 (1984)
- [17] MYNICK, H.E., Princeton Plasma Physics Laboratory Report PPPL-2856 (1992)

- [18] SIGMAR, D.J. and HSU, C.T., WHITE, R.B, and CHENG, C.Z, Phys. Fluids B4, 1506 (1992)
- [19] BITTONI, E. and HAEGI, M., Fusion Technology 22, Dec. 1992
- [20] MYNICK, H.E., Bull. Am. Phys. Soc. 37, to be published in Phys. Fluids 1993
- [21] HSU, C.T. and SIGMAR, D.J., MIT, Personal communication (1992)
- [22] BUDNY, R.V., et al, Nucl. Fus.32, 429 (1992)
- [23] SCHIVELL, J. et al, Rev. sci., Inst. 63, 4760 (1992)
- [24] JOHNSON, L. et al, Rev. Sci. Inst. 63, 4517 (1992)
- [25] STRATTON, B.C, FONCK, R.J et al, Rev. Sci. Inst. 63, 5179 (1992)
- [26] FISHER, R.K., et al, Rev. Sci. Inst. 63, 4499 (1992)
- [27] RHEE, D.Y., et al, Rev. Sci. Inst. 63, 4644 (1992)
- [28] CHENG, C.Z. et al, this conference
- [29] BIGLARI, H. et al, Phys Fluids B4, 2385 (1992)
- [30] BIGLARI, H. and CHEN, L., Phys. Rev. Lett 67, 3681 (1991)
- [31] POST, D.E., et al, ITER Physics, ITER Documentation Series No. 21, to be published by the IAEA, Vienna, 1991
- [32] SCOTT, S. et al, Proc. 13th Int'l. Conf. on Plasma Physics and Controlled Nucl Fusion Research, Washington, D.C., IAEA Vienna, 1990, p. 235
- [33] REBUT, P.H., ibid, p. 27
- [34] JACQUINOT, J., ibid, p. 679

**Table 1**

<u>Alpha Loss Mechanism</u>	<u>Alpha Loss Fraction in TFTR D-T (est.)</u>	<u>Alpha Loss Fraction in ITER (rough est.)</u>
First-orbit	≈5-50%[2]	<1%
Stochastic TF Ripple	≈1-5%[3]	≈1%[31]
Plasma Turbulence	<1%[2]	<1%
Plasma-driven MHD	≤10-30%	≈1-3%
Sawtooth crash	<<1%	<<1%
Pre-disruptive MHD	≈1-10%	≤1%
Delayed loss	≈1-10%	≈1-10%(?)
ICRF induced	≈1-10%	≈1%(?)

**Table 1:** Single particle loss mechanism observed for alpha-like D-D fusion products (and other fast ions) in TFTR, along with rough estimates for their effects on global alpha loss in TFTR D-T and ITER. The values for TFTR come from a mixture of experiment, modeling, and theory, and are uncertain by at least a factor of 2-3. The MHD induced loss estimates for ITER are based on the TFTR estimates plus modeling of MHD-induced losses vs.  $\rho_{\alpha}/a$ .

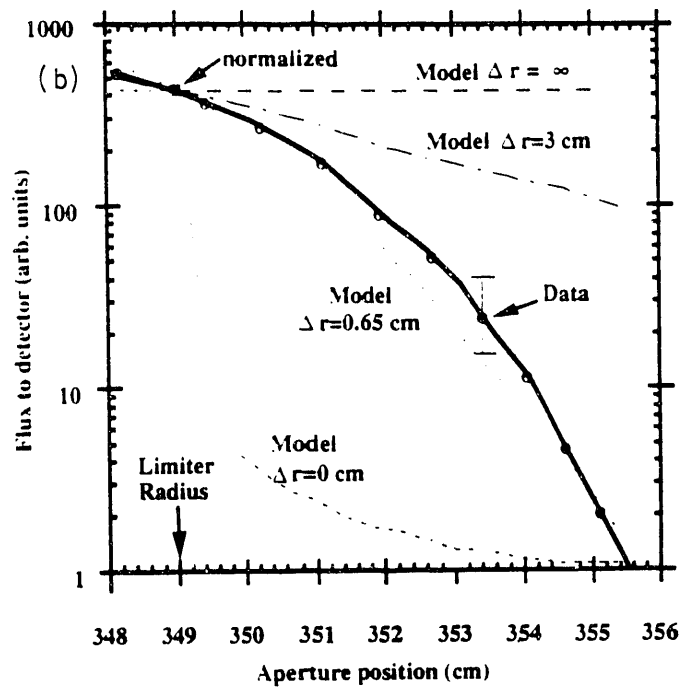
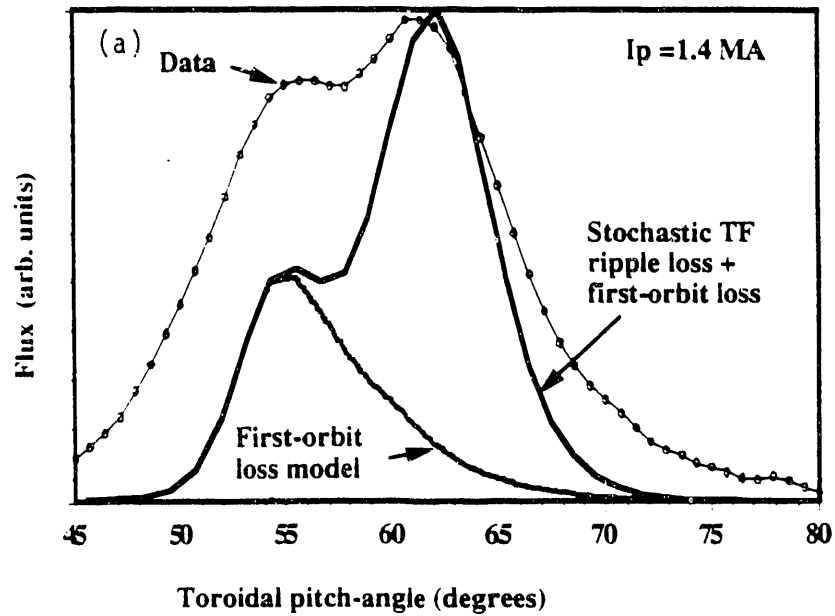


Fig. 1 -- Part (a) shows the pitch angle distribution of D-D fusion product loss to the  $20^\circ$  (midplane) probe in a plasma with  $I_p = 1.4$  MA,  $R = 2.6$  m,  $a = 0.95$  m, and  $B = 4$  T. The location of the peak at  $\chi \approx 62^\circ$  is approximately consistent with the stochastic TF ripple diffusion model. Part (b) shows the D-D fusion product loss to the midplane probe (at  $\chi = 60^\circ$ ) vs. the major radius of the probe aperture in a plasma with  $I_p = 1.6$  MA,  $R = 2.45$  m,  $a = 0.8$  m, and  $B = 5$  T. The shape of the radial profile behind the projected position of the RF limiter is also consistent with the stochastic TF ripple model, which predicts a step size of  $\Delta r = 0.75$  cm for these orbits.

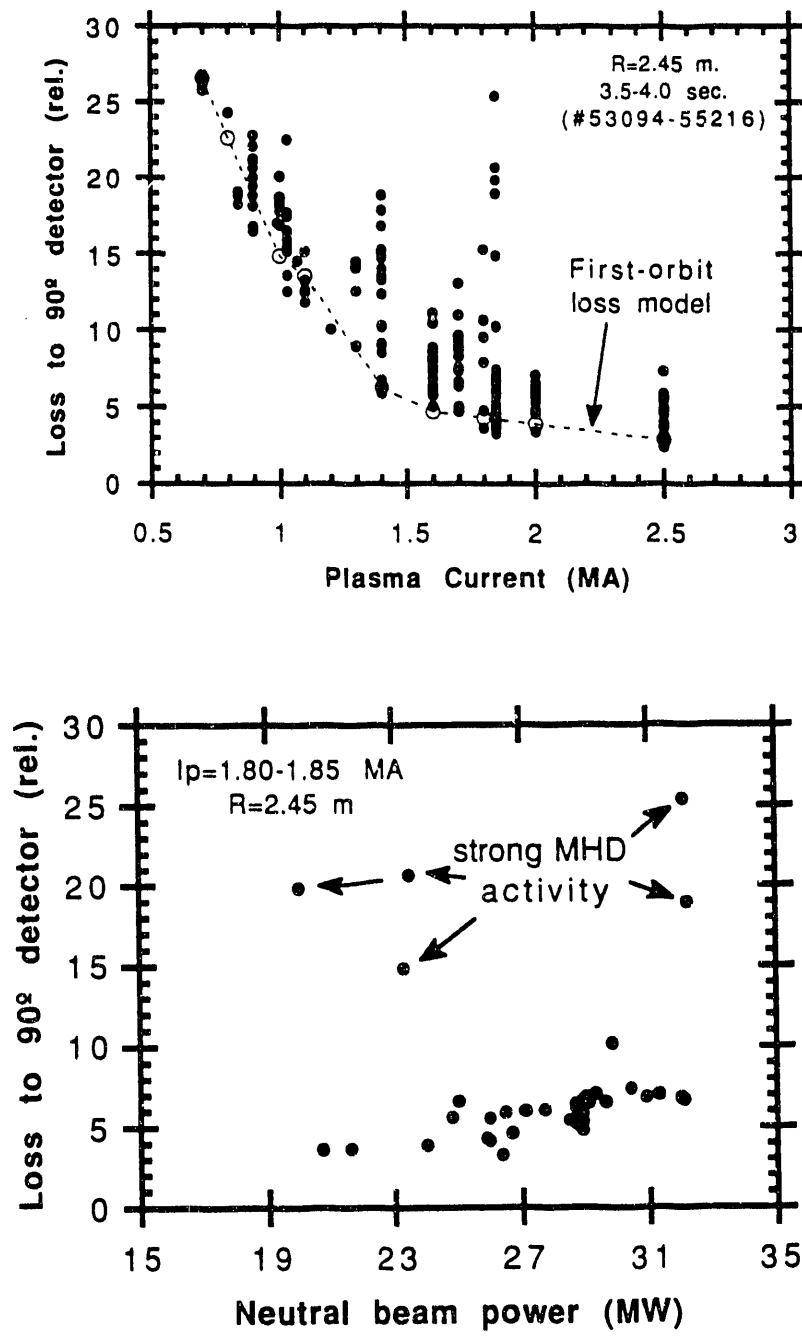
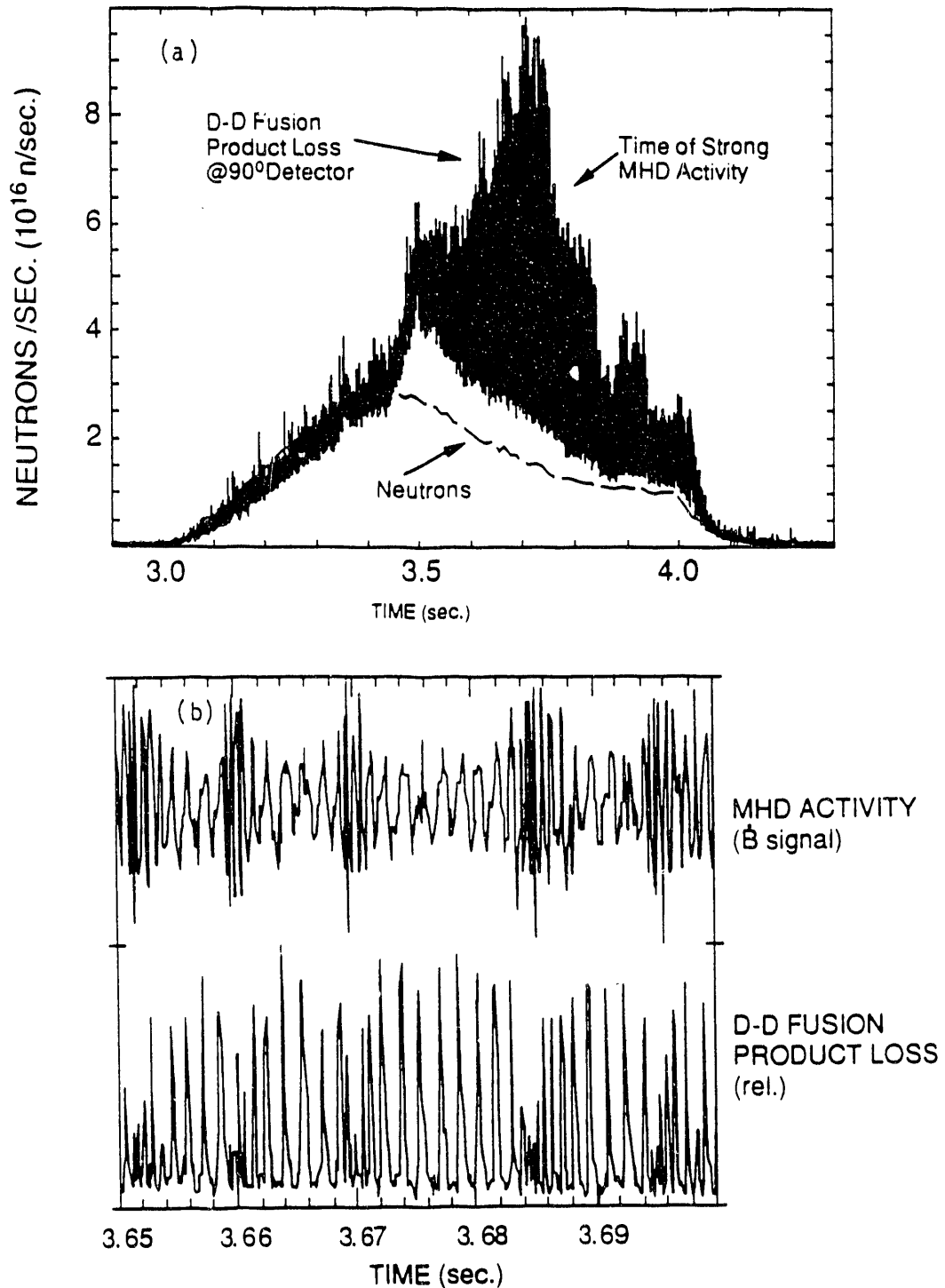
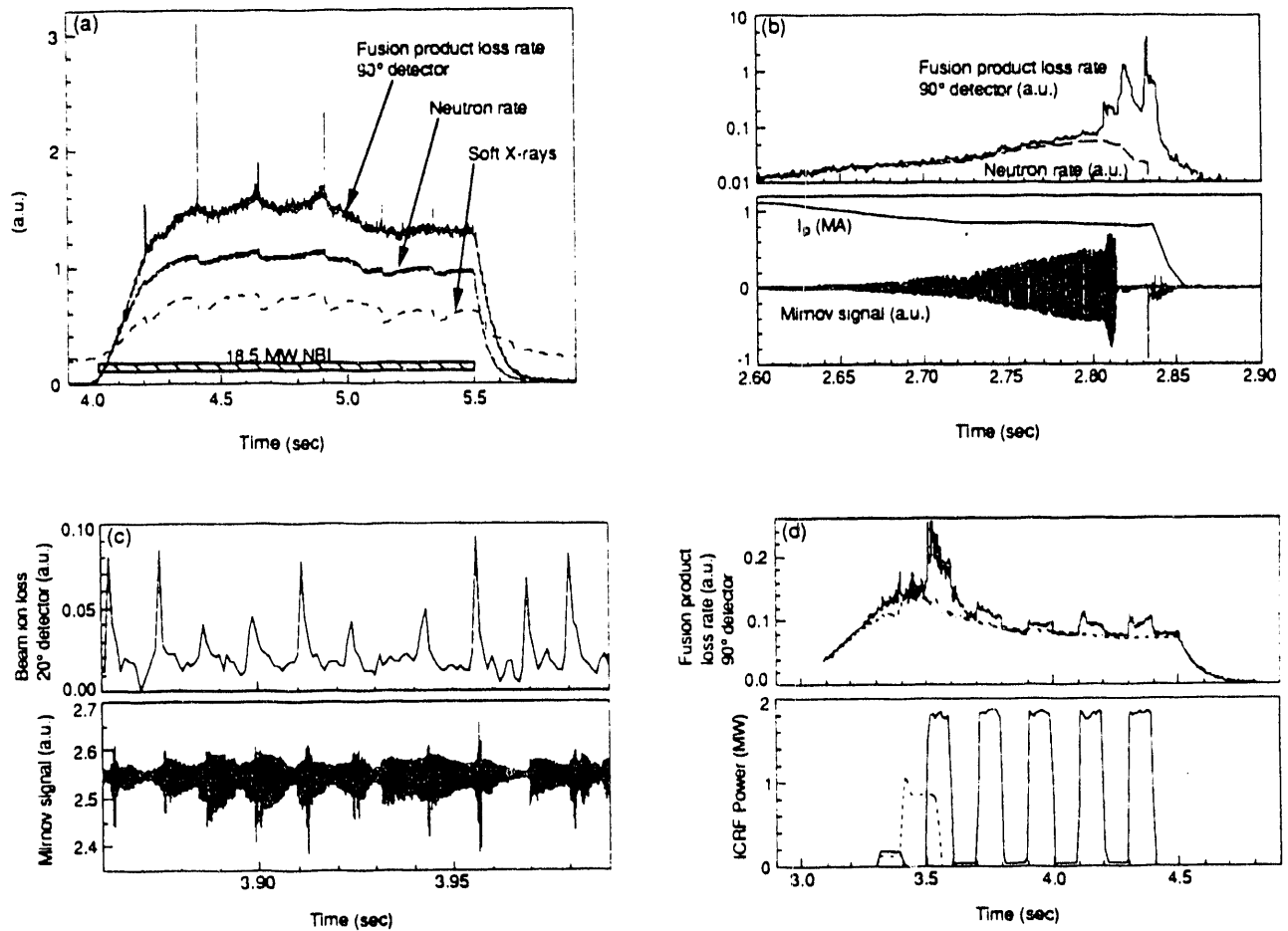


Fig. 2 -- Part (a) shows the D-D fusion product loss to 90° detector (normalized to the neutron source rate) vs. plasma current for a set of ≈200 TFTR discharges with P = 5-32 MW of NBI. The loss is integrated over 3.5-4.0 sec (with NBI from 3-4 sec). The curve represents the calculated first-orbit loss, which was normalized to the data at the lowest current point where the first-orbit loss is expected to dominate. Part (b) shows the same loss for the Ip = 1.80-1.85 MA cases of part (a) vs. the NBI power. The normalized loss is largest for the discharges in which strong coherent MHD activity modulates the loss, but it also increases gradually with increasing NBI power (and neutron rate).



**Fig. 3** -- An example of MHD induced loss of D-D fusion products to the  $90^\circ$  detector for a discharge with  $I_p = 1.4$  MA,  $R = 2.45$  m,  $a = 0.8$  m, and  $P = 24$  MW of NBI from 3-4 sec (#48367). Part (a) shows that the fusion product loss increases at  $\approx 3.5$  sec, which coincides with the onset of strong MHD activity and a drop in the neutron rate. Note that the D-D fusion product loss signal is normalized to match the neutron rate in a similar discharge without MHD (at  $P = 20$  MW). Part (b) is a 5 msec portion of the discharge in (a) showing the modulation of the D-D fusion product loss at the frequency of the Mirnov oscillations. During this time there are (1,1) and (2,1) modes with  $\bar{B}_r/B_T \approx 3 \times 10^{-4}$ .



**Fig. 4** -- Other examples of MHD induced and ICRF induced loss of D-D fusion products and other fast ions, as monitored by a PM tube viewing the total scintillator light emission vs time. Part (a) shows a rapid increase in the D-D fusion product loss rate to the 90° detector during sawtooth crashes (#66218), typically observed over  $I_p = 1-2$  MA. Part (b) shows a x50 increase in the D-D fusion product loss to the 90° detector during pre-disruptive MHD activity (#66088). Part (c) shows the loss of 100 keV neutral beam ions to the 20° detector coincident with ABM activity in a low-field discharge (#58625). Part (d) shows an apparent ICRF induced loss of D-D fusion products to the 90° detector, which occurred during an ICRF electron heating experiment with NBI, but without any minority species present (#66341).

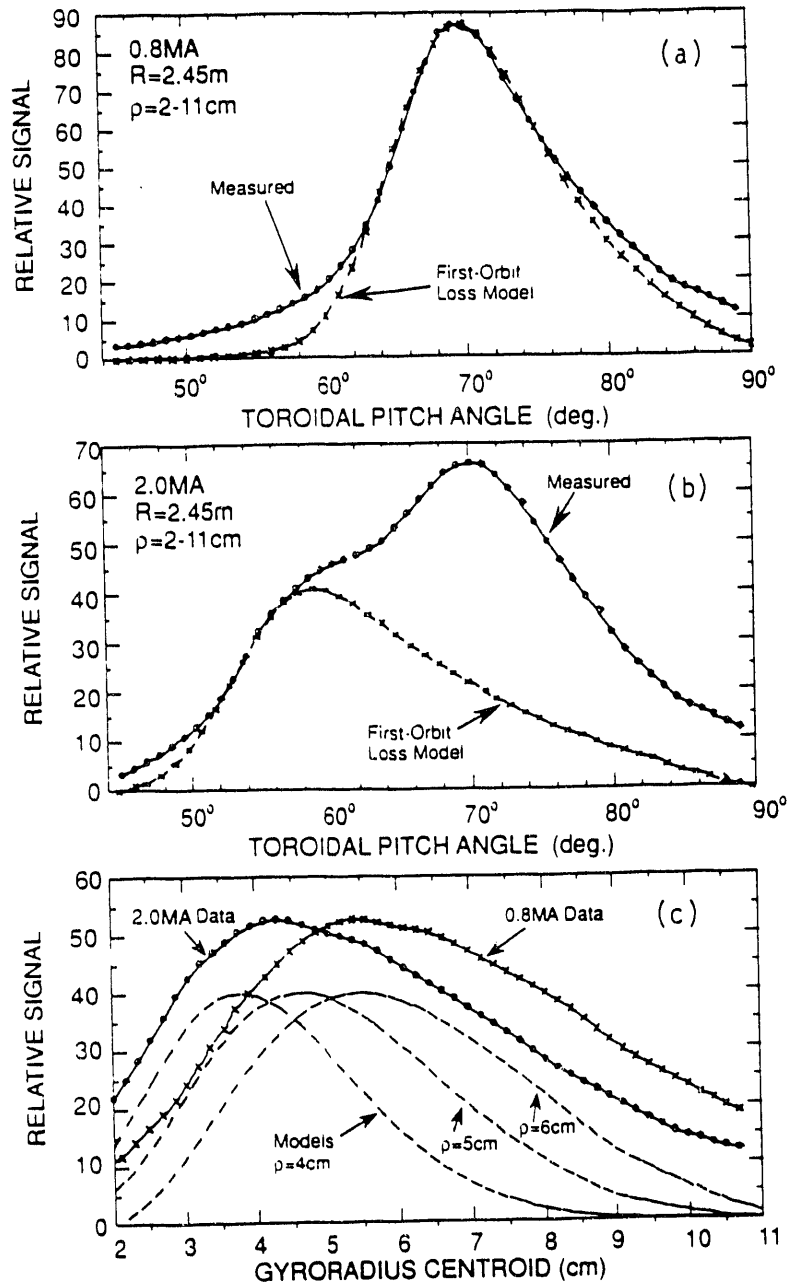


**Fig. 5** -- Pitch angle distributions of D-D fusion product loss to the  $90^\circ$  detector inferred from the scintillator images, averaged over 3.5-4.0 sec (with NBI from 3-4 sec). In (a) is an  $I_p = 0.8$  MA case (#54454) and in (b) is a 2.0 MA case (#55050), both for  $R = 2.45$  m plasmas at  $B = 4.8$  T. At 2.0 MA there is an anomalous loss feature at  $\chi \approx 70^\circ$  which increases with NBI power (with respect to first-orbit loss), while at 0.8 MA the data is consistent with first-orbit loss. At intermediate currents the first-orbit loss peak moves to lower pitch angles while the anomalous feature remains at  $\chi \approx 70^\circ$ . The corresponding gyroradius distributions for the cases in (a) are shown in Fig. 5(c). The distribution at 0.8 MA case is consistent with the model curve for  $\rho \approx 6$  cm, about as expected for first-orbit loss of D-D fusion products at their birth energy. However, the distribution at 2.0 MA is more consistent with  $\rho \approx 4-5$  cm, implying loss at an energy  $E/E_0 \approx 55 \pm 15\%$  times the birth energy.

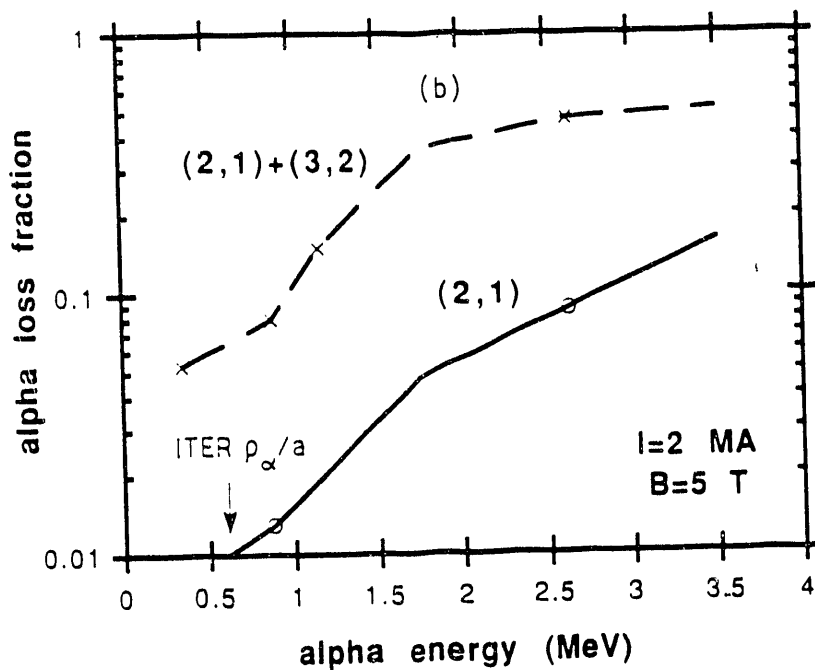
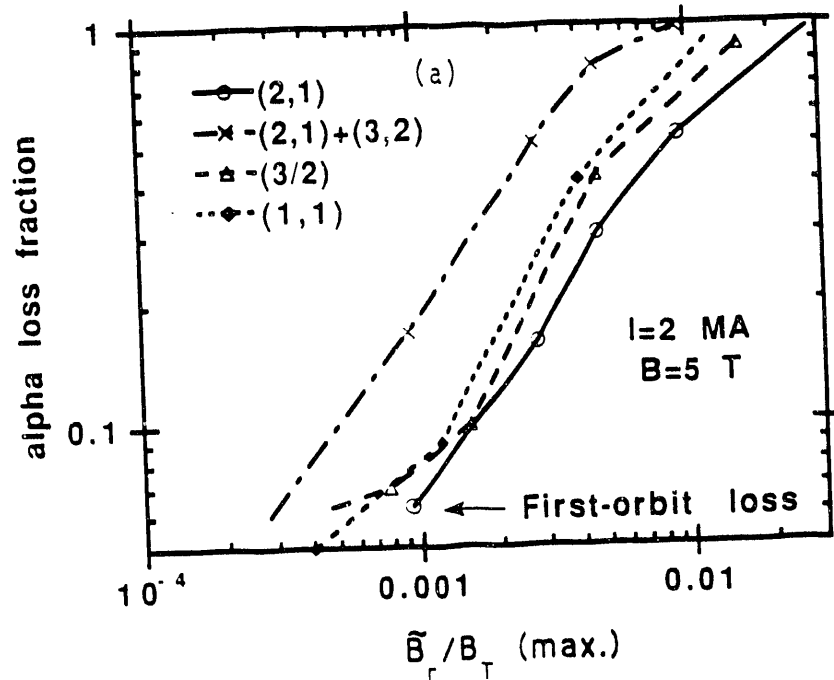


Fig. 6 -- Modeling of the global alpha particle loss fraction for a TFTR plasma with  $I_p = 2$  MA and  $B = 5$  T. In (a) the amplitude and mode number is varied for 3.5 MeV alphas, while in (b) the assumed alpha energy is varied for two of the amplitudes of (a). The calculated MHD-induced loss becomes comparable to the first-orbit loss at  $\tilde{B}_r/B_T \approx 2-3 \times 10^{-3}$  for single-helicity modes. Note that the horizontal scale for the  $(3,2)+(2,1)$  case refers to the  $(2,1)$  amplitude only, not including the 1.6 times larger  $(3,2)$  amplitude. The loss of 3.5 MeV alphas in an ITER sized (but circular) machine is roughly equivalent to the loss of  $\approx 0.6$  MeV alphas (or D-D fusion products) in TFTR.

EXTERNAL DISTRIBUTION IN ADDITION TO UC-420

Dr. F. Paoloni, Univ. of Wollongong, AUSTRALIA  
 Prof. M.H. Brennan, Univ. of Sydney, AUSTRALIA  
 Plasma Research Lab., Australian Nat. Univ., AUSTRALIA  
 Prof. I.R. Jones, Flinders Univ, AUSTRALIA  
 Prof. F. Cap, Inst. for Theoretical Physics, AUSTRIA  
 Prof. M. Heindler, Institut für Theoretische Physik, AUSTRIA  
 Prof. M. Goossens, Astronomisch Instituut, BELGIUM  
 Ecole Royale Militaire, Lab. de Phy. Plasmas, BELGIUM  
 Commission-European, DG. XII-Fusion Prog., BELGIUM  
 Prof. R. Bouciqué, Rijksuniversiteit Gent, BELGIUM  
 Dr. P.H. Sakonaka, Instituto Fisica, BRAZIL  
 Instituto Nacional De Pesquisas Espaciais-INPE, BRAZIL  
 Documents Office, Atomic Energy of Canada Ltd., CANADA  
 Dr. M.P. Bachynski, MPB Technologies, Inc., CANADA  
 Dr. H.M. Skarsgard, Univ. of Saskatchewan, CANADA  
 Prof. J. Teichmann, Univ. of Montreal, CANADA  
 Prof. S.R. Sreenivasan, Univ. of Calgary, CANADA  
 Prof. T.W. Johnston, INRS-Energie, CANADA  
 Dr. R. Bolton, Centre canadien de fusion magnétique, CANADA  
 Dr. C.R. James, Univ. of Alberta, CANADA  
 Dr. P. Lukáč, Komenského Univerzita, CZECHO-SLOVAKIA  
 The Librarian, Culham Laboratory, ENGLAND  
 Library, R61, Rutherford Appleton Laboratory, ENGLAND  
 Mrs. S.A. Hutchinson, JET Library, ENGLAND  
 Dr. S.C. Sharma, Univ. of South Pacific, FIJI ISLANDS  
 P. Mähönen, Univ. of Helsinki, FINLAND  
 Prof. M.N. Bussac, Ecole Polytechnique, FRANCE  
 C. Mouttet, Lab. de Physique des Milieux Ionisés, FRANCE  
 J. Radet, CEN/CADARACHE - Bat 506, FRANCE  
 Prof. E. Economou, Univ. of Crete, GREECE  
 Ms. C. Rinni, Univ. of Ioannina, GREECE  
 Dr. T. Mui, Academy Bibliographic Ser., HONG KONG  
 Preprint Library, Hungarian Academy of Sci., HUNGARY  
 Dr. B. DasGupta, Saha Inst. of Nuclear Physics, INDIA  
 Dr. P. Kaw, Inst. for Plasma Research, INDIA  
 Dr. P. Rosensau, Israel Inst. of Technology, ISRAEL  
 Librarian, International Center for Theo Physics, ITALY  
 Miss C. De Palo, Associazione EURATOM-ENEA, ITALY  
 Dr. G. Grosso, Istituto di Fisica del Plasma, ITALY  
 Prof. G. Rostangni, Istituto Gas Ionizzati Del Cnr, ITALY  
 Dr. H. Yamato, Toshiba Res & Devel Center, JAPAN  
 Prof. I. Kawakami, Hiroshima Univ., JAPAN  
 Prof. K. Nishikawa, Hiroshima Univ., JAPAN  
 Director, Japan Atomic Energy Research Inst., JAPAN  
 Prof. S. Itoh, Kyushu Univ., JAPAN  
 Research Info. Ctr., National Inst. for Fusion Science, JAPAN  
 Prof. S. Tanaka, Kyoto Univ., JAPAN  
 Library, Kyoto Univ., JAPAN  
 Prof. N. Inoue, Univ. of Tokyo, JAPAN  
 Secretary, Plasma Section, Electrotechnical Lab., JAPAN  
 S. Mori, Technical Advisor, JAERI, JAPAN  
 Dr. O. Mitarai, Kumamoto Inst. of Technology, JAPAN  
 J. Hyeon-Sook, Korea Atomic Energy Research Inst., KOREA  
 D.I. Choi, The Korea Adv. Inst. of Sci. & Tech., KOREA  
 Prof. B.S. Liley, Univ. of Waikato, NEW ZEALAND  
 Inst of Physics, Chinese Acad Sci PEOPLE'S REP. OF CHINA  
 Library, Inst. of Plasma Physics, PEOPLE'S REP. OF CHINA  
 Tsinghua Univ. Library, PEOPLE'S REPUBLIC OF CHINA  
 Z. Li, S.W. Inst Physics, PEOPLE'S REPUBLIC OF CHINA  
 Prof. J.A.C. Cabral, Instituto Superior Tecnico, PORTUGAL  
 Dr. O. Petrus, AL I CUZA Univ., ROMANIA  
 Dr. J. de Villiers, Fusion Studies, AEC, S. AFRICA  
 Prof. M.A. Hellberg, Univ. of Natal, S. AFRICA  
 Prof. D.E. Kim, Pohang Inst. of Sci. & Tech., SO. KOREA  
 Prof. C.I.E.M.A.T, Fusion Division Library, SPAIN  
 Dr. L. Stenflo, Univ. of UMEA, SWEDEN  
 Library, Royal Inst. of Technology, SWEDEN  
 Prof. H. Wilhelmson, Chalmers Univ. of Tech., SWEDEN  
 Centre Phys. Des Plasmas, Ecole Polytech, SWITZERLAND  
 Bibliotheek, Inst. Voor Plasma-Fysica, THE NETHERLANDS  
 Asst. Prof. Dr. S. Cakir, Middle East Tech. Univ., TURKEY  
 Dr. V.A. Glukhikh, Sci. Res. Inst. Electrophys. Apparatus, USSR  
 Dr. D.D. Ryutov, Siberian Branch of Academy of Sci., USSR  
 Dr. G.A. Eliseev, I.V. Kurchatov Inst., USSR  
 Librarian, The Ukr.SSR Academy of Sciences, USSR  
 Dr. L.M. Kovrizhnykh, Inst. of General Physics, USSR  
 Kernforschungsanlage GmbH, Zentralbibliothek, W. GERMANY  
 Bibliothek, Inst. Für Plasmaforschung, W. GERMANY  
 Prof. K. Schindler, Ruhr-Universität Bochum, W. GERMANY  
 Dr. F. Wagner, (ASDEX), Max-Planck-Institut, W. GERMANY  
 Librarian, Max-Planck-Institut, W. GERMANY  
 Prof. R.K. Janev, Inst. of Physics, YUGOSLAVIA

**END**

---

**DATE  
FILMED**

6 / 23 / 93

